Analytical systematic approximate method of a two-state dissipative system

Ke-lin Wang, Wei Jiang, Shao-long Wan, and Hai-jun Pan
Center of Nonlinear Science, Department of Astronomy and Applied Physics, University of Science and Technology of China, Hefei 230026, China

(Received 1 July 1999; revised manuscript received 7 December 1999)

Occupation probability and changes of the environment in a dissipative two-state system have been investigated using a systematic approximate method. This method explores the tunneling dynamics through a system state vector with manifest physical meanings and provides a deep microscopic insight into the dynamical behaviors of the system.

PACS number(s): 02.70.−c, 03.65.−w

I. INTRODUCTION

A problem that is of general interest in both physics and chemistry is that of a quantum mechanical system tunneling between two states and subjects to a dissipative coupling to environment degree of freedom. Examples of this type of system abound; they include the tunneling of defects in metallic glasses [1], and the motion of the total flux in a superconducting quantum interference device between two metastable fluxoid states [2]. One of the most intriguing features of this model is a dynamical phase transition between coherent tunneling and incoherent relaxation. This was first predicted by Chakravarty and co-workers [3,4], and later confirmed by experiments on interstitial tunneling in niobium [5].

A great deal of work has been carried out over the last ten years in order to understand the dynamics of this apparently simple model. Extensive calculations based on the Feyman-Vernon path integral formalism within the NIBA have yielded reliable information for weak dissipation [4]. In addition to such direct attempts at calculating dynamics for the spin-boson model, it has proved fruitful to exploit analogies between this model and several other models, including the inverse-square Ising model [6], and the anisotropic Kondo model [7]. It has been shown that the partition functions of these different models can be put into correspondence and the parameters of the models related. This connection enables us to determine the thermodynamics of this model from quantum Monte Carlo method (QMC).

But most QMC simulations fail to give a detailed microscopic analysis to the interaction between the system and environment, especially to variations of the environment. In this paper, we describe a systematic approximate method for calculating the real-time dynamics of dissipative quantum systems and use it to investigate the dynamical behaviors at zero temperature. Since we can give the result in analytic form, this method draws out a clear microscopic physical picture for the system dynamics through a system-environment state vector based on a set of resonable suppositions. It not only predicts the transition from coherence to incoherence accurately, but also simulates the energy transfer between environment and the system successfully.

Dissipative two-state systems are often described by the spin-boson model:

$$H=-\Delta\sigma_x+\frac{\epsilon}{2}\sigma_z+\sum_i \omega_i\left(a_i^+a_i+\frac{1}{2}\right)+\sigma_z\sum_i A_i(\omega_i)(a_i^++a_i). \tag{1}$$

Here $\sigma_i, i=x,y,z$ are Pauli spin matrices, the two states of the system correspond to $\sigma_z=1$ and $\sigma_z=-1$ is the bare tunneling matrix element and ϵ is a bias. The environment is represented by an infinite set of harmonic oscillators (labeled by the index i) with m_i and frequency spectrum ω_i coupling linearly to the coordinate $Q=A_i(\omega_i)\sigma_z$ of the two-state system, where $A_i(\omega_i)=\frac{1}{2}(c_i/\sqrt{2m_i\omega_i})$ and c_i is the coupling to the ith oscillator. We restrict our discussion of the model to the zero and so-called Ohmic regime, where the spectral density of the environment is given by $J(\omega)=2\pi\alpha\exp(-\omega/\omega_c)$, with ω_c being the high energy cutoff and α the dimensionless parameter characterizing the strength of the dissipation. The scaling limit $\omega_c\gg\Delta$ is characteristic of tunneling in solids and, as shown by scaling argument [8,9], the Ohmic spin-boson model has nontrivival dynamics only for $\alpha<1$ and renormalized tunneling frequency $\Delta_r=\Delta(\Delta/\omega_c)^{\alpha(1-\alpha)}$ is the only frequency scale of the dynamics at zero temperature other than ω_c.

II. DISCUSSION OF DYNAMICAL BEHAVIORS

In particular, we suppose the phonon is the energy quanta of the environment so that the enviroment now is regarded as an infinite phonon bath in which most phonons are in ground state and the transition from coherence to incoherence is in fact a process that decreasing system energy makes a certain number of phonons in ground state excited. The system is initially held in $\sigma_z=1$ for some large negative time. This can be achieved by applying a strong bias for $t<0$. At time zero the constraint is released and for $t>0$ the dynamics is governed by the spin-phonon Hamitonian. In the direction of this idea, we resolve several physical quantities and give a relevant discussion about their dynamical behaviors for small coupling strength $(0<\alpha<0.5)$.

Omitting the term $\Sigma_i \frac{1}{2}\omega_i$ in Eq. (1), we rewrite the spin-phonon Hamitonian as

$$H=-\Delta\sigma_x+\frac{\epsilon}{2}\sigma_z+\sum_i \omega_i a_i^+ a_i+\sigma_z\sum_i A_i(a_i^+ + a_i). \tag{2}$$

According to the previous discussion, here the term $\Sigma_i \omega_i a_i^+ a_i$ represents the excited phonon energy and $\sigma_z\Sigma_i(a_i^+ + a_i)$ does the interaction between system and excited phonons. We also notice that in the Hamitonian (2) there are two marked features: the phonon number is not conservative; there is linear term of a_i, a_i^+. So the solution of coherent form may be suitable for Hamitonian (2). Meanwhile, the dissipative interaction's being weak effect and the spin independence of electron-phonon interaction are considered. Finally, we suppose the approximate state vector of the whole system and environment as

$$|t\rangle=\begin{pmatrix} f_1(t)+\sum_i g_i(t)a_i^+ \\ f_2(t)+\sum_i g_i(t)a_i^+ \end{pmatrix}|\rangle \tag{3}$$

where $|\rangle$ denotes $\exp[\Sigma_j \alpha_j(t)a_j^+]|0\rangle$, which has the basic properties $a_j|\rangle=\alpha_j|\rangle$, $\langle|a_j^+=\langle|\alpha_j^*$; the average phonon number in coherent state is $\langle|a_j^+ a_j|\rangle=|\alpha|^2$ [10], and $g_i(t)$ is the spin-phonon coupling strength. At $t\leqslant 0$, there are so few excited phonons that $g_i(t)|_{t=0}\doteq 0, \alpha_j(t)|_{t=0}\doteq 0$. $\alpha_j(t), g_i(t), f_1(t), f_2(t)$ are to be determined by the Schrödinger equation as follows.

Substituting $|t\rangle$ into the Schrödiger equation $\imath(\partial/\partial t)|t\rangle = H|t\rangle$ and making an approximation omitting $a_i^+ a_j^+|\rangle$ terms, we get

$$\imath\frac{\partial}{\partial t}|\rangle\doteq\imath\begin{pmatrix} \dot f_1(t)+\sum_i [\dot g_i(t)+f_1(t)\dot\alpha_i(t)]a_i^+ \\ \dot f_2(t)+\sum_i [\dot g_i(t)+f_2(t)\dot\alpha_i(t)]a_i^+ \end{pmatrix}|\rangle, \tag{4}$$

$$H|t\rangle\doteq-\Delta\begin{pmatrix} f_2(t)+\sum_i g_i(t)a_i^+ \\ f_1(t)+\sum_i g_i(t)a_i^+ \end{pmatrix}|\rangle+\frac{\epsilon}{2}\begin{pmatrix} f_1(t)+\sum_i g_i(t)a_i^+ \\ -f_2(t)-\sum_i g_i(t)a_i^+ \end{pmatrix}|\rangle+\begin{pmatrix} \sum_i \omega_i f_1(t)\alpha_i(t)a_i^+ +\sum_i \omega_i g_i(t)a_i^+ \\ \sum_i \omega_i f_2(t)\alpha_i(t)a_i^+ +\sum_i \omega_i g_i(t)a_i^+ \end{pmatrix}|\rangle$$
$$+\begin{pmatrix} \sum_i f_1(t)A_i a_i^+ \\ -\sum_i f_2(t)A_i a_i^+ \end{pmatrix}|\rangle+\begin{pmatrix} \sum_i A_i[f_1(t)\alpha_i(t)+g_i(t)]+\sum_{ij} A_j\alpha_j(t)g_i(t)a_i^+ \\ -\sum_i A_i[f_2(t)\alpha_i(t)+g_i(t)]-\sum_{ij} A_j\alpha_j(t)g_i(t)a_i^+ \end{pmatrix}|\rangle. \tag{5}$$

Comparing corresponding coefficients of $|\rangle$, $a_i^+|\rangle$ terms and making $\phi_1(t)=f_1(t)+f_2(t), \phi_2(t)=f_1(t)-f_2(t)$, we obtain the following self-contained relations:

$$\imath\dot\phi_1(t)=-\Delta\phi_1(t)+\frac{\epsilon}{2}\phi_2(t)+\sum_i A_i\phi_2(t)\alpha_i(t), \tag{6}$$

$$\imath\dot\phi_2(t)=\Delta\phi_2(t)+\frac{\epsilon}{2}\phi_1(t)+\sum_i A_i[\phi_1(t)\alpha_i(t)+2g_i(t)], \tag{7}$$

$$\imath\phi_2(t)\dot\alpha_j(t)=\epsilon g_j(t)+\omega_j\alpha_j(t)\phi_2(t)+A_j\phi_1(t)+2g_j(t)\sum_i \alpha_i(t)A_i, \tag{8}$$

$$2\imath\dot g_j(t)=-2\Delta g_j(t)+2\omega_j g_j(t)+\omega_j\phi_1(t)\alpha_j(t)+A_j\phi_2(t)-\imath\phi_1(t)\dot\alpha_j(t). \tag{9}$$

Because the phonon bath possesses infinite degrees of freedom, it is reasonable to adopt the transformation $\Sigma_i \to \int J(\omega)d\omega, A_i\to A(\omega), g_i(t)\to g(\omega,t), \alpha_i(t)\to\alpha(\omega,t)$. After the transformation, we get the following group of differential-integrate equations:

$$\imath\dot\phi_1(t)=-\Delta\phi_1(t)+\frac{\epsilon}{2}\phi_2(t)+\int A(\omega)\phi_2(t)\alpha(\omega,t)J(\omega)d\omega, \tag{10}$$

$$\imath\dot\phi_2(t)=\Delta\phi_2(t)+\frac{\epsilon}{2}\phi_1(t)+\int A(\omega)[\phi_1(t)\alpha(\omega,t)+2g(\omega,t)]J(\omega)d\omega, \tag{11}$$

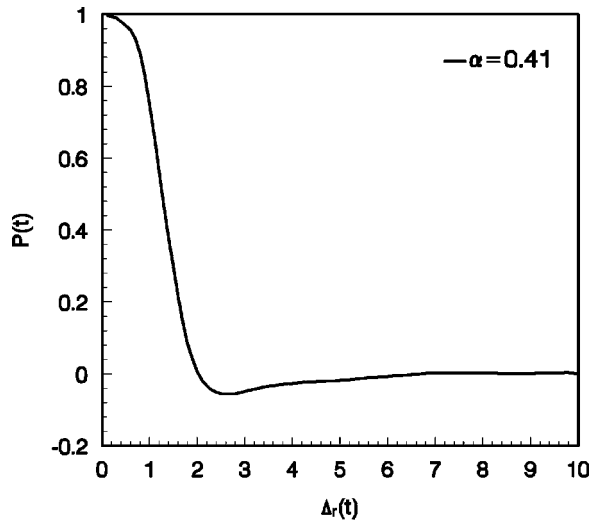

FIG. 1. $P(t)$ at $\alpha-0.41$ and $T=0$ in the case that only the first order effect is considered. Here the data are for $\Delta/\omega_c=1/50$, $\epsilon=0$.

$$\imath\phi_2(t)\dot{\alpha}(\omega,t)=\epsilon g(\omega,t)+\omega\alpha(\omega,t)\phi_2(t)+A(\omega,t)\phi_1(t)+2g(\omega,t)\int\alpha(\omega,t)A(\omega)J(\omega)d\omega, \quad (12)$$

$$2\imath\dot{g}(\omega,t)=-2\Delta g(\omega,t)+2\omega g(\omega,t)+\omega\phi_1(t)\alpha(\omega,t)+A(\omega,t)\phi_2(t)-\imath\phi_1(t)\dot{\alpha}(\omega,t). \quad (13)$$

The dynamical quantity which is most directly relevant in the phenomena of ''macroscopic quantum coherence'' is the expectation value of $\langle\sigma_z\rangle$, namely, occupation probability $p(t)=\langle\sigma_z\rangle$ [11]. The analytic expression for $p(t)$ is $C_1(t)/D_1(t)$, here

$$C_1(t)=f_1(t)f_1^*(t)-f_2(t)f_2^*(t)+[f_1^*(t)-f_2^*(t)]\int g(\omega,t)\alpha^*(\omega,t)J(\omega)d\omega+[f_1(t)-f_2(t)]\int g^*(\omega,t)\alpha(\omega,t)J(\omega)d\omega, \quad (14)$$

$$D_1(t)=f_1(t)f_1^*(t)+f_2(t)f_2^*(t)+[f_1^*(t)+f_2^*(t)]\int g(\omega,t)\alpha^*(\omega,t)J(\omega)d\omega+[f_1(t)+f_2(t)]\int g^*(\omega,t)\alpha(\omega,t)J(\omega)d\omega+2\int g^*(\omega,t)g(\omega,t)J(\omega)d\omega. \quad (15)$$

Figure 1 shows the numerical result for $p(t)$ at zero temperature and for $\alpha=0.41$, where the oscillations disappear completely. Past that value, we are not able to resolve $p(t)$ correctly. Comparing Fig. 1 with the result of NIBA [12], we find no qualitive differentiation between them. But the value has obvious divergence from the Toulouse limit ($\alpha_c=0.5$). This dissatisfying result can be explained by the form of the state vector $|t\rangle$. Since the ratio of the contribution of the second order effect to that of first order at the critical point is about 0.20, which is not a small quantity, the form of $|t\rangle$ is not accurate enough. To tackle this problem, the second spin-phonon interaction is taken into account. $|t\rangle$ now can be written as

$$|t\rangle=\begin{pmatrix} f_1(t)+\sum_i g_{1i}(t)a_i^+ +\sum_{ij} h_{ij}(t)a_i^+a_j^+ \\ f_2(t)+\sum_i g_{2i}(t)a_i^+ +\sum_{ij} h_{ij}(t)a_i^+a_j^+ \end{pmatrix}|\rangle. \quad (16)$$

Again, the parameters in the state vector are to be determined by the same method. After a series of derivations similiar to those in the case of the state vector (3), the following equations are obtained:

$$\imath\dot{f}_1(t)=-\Delta f_2(t)+\frac{\epsilon}{2}f_1(t)+\int A(\omega)[f_1(t)\alpha(\omega,t)+g_1(\omega,t)]J(\omega)d\omega, \quad (17)$$

$$\imath\dot{f}_2(t)=-\Delta f_1(t)-\frac{\epsilon}{2}f_2(t)-\int A(\omega)[f_2(t)\alpha(\omega,t)+g_2(\omega,t)]J(\omega)d\omega, \quad (18)$$

$$\imath[\dot{g}_1(\omega,t)+f_1(t)\dot{\alpha}(\omega,t)]=-\Delta g_2(\omega,t)+\frac{\epsilon}{2}g_1(\omega,t)+\omega[g_1(\omega,t)+f_1(t)\times\alpha(\omega,t)]+A(\omega)f_1(t)+\int A(\omega)g_1(\omega,t)\alpha\times(\omega,t)J(\omega)d\omega+\int[h(\omega,\omega_1,t)+h(\omega_1,\omega,t)]\times A(\omega_1)J(\omega_1)d\omega_1, \quad (19)$$

$$\imath[\dot{g}_2(\omega,t)+f_2(t)\dot{\alpha}(\omega,t)]=-\Delta g_1(\omega,t)-\frac{\epsilon}{2}g_2(\omega,t)+\omega[g_2(\omega,t)+f_2(t)\times\alpha(\omega,t)]-A(\omega)f_2(t)-\int A(\omega_1)\alpha(\omega_1,t)g_2(\omega,t)\times J(\omega_1)d\omega_1-\int[h(\omega,\omega_1,t)+h(\omega_1,\omega,t)]\times A(\omega_1)J(\omega_1)d\omega_1, \quad (20)$$

$$\imath[\dot{h}(\omega_1,\omega_2,t)+g_1(\omega_1,t)\dot{\alpha}(\omega_2,t)]=-\Delta h(\omega_1,\omega_2,t)+\frac{\epsilon}{2}h(\omega_1,\omega_2,t)+\omega_1[h(\omega_1,\omega_2,t)+h(\omega_2,\omega_1,t)]+\omega_1\alpha(\omega_1,t)g_1(\omega_2,t)+A(\omega_1)g_1(\omega_2,t)+h(\omega_1,\omega_2,t)\int A(\omega)\alpha(\omega,t)J(\omega)d\omega, \quad (21)$$

$$\imath[\dot{h}(\omega_1,\omega_2,t)+g_2(\omega_1,t)\dot{\alpha}(\omega_2,t)]=-\Delta h(\omega_1,\omega_2,t)-\frac{\epsilon}{2}h(\omega_1,\omega_2,t)+\omega_1[h(\omega_1,\omega_2,t)+h(\omega_2,\omega_1,t)]$$
$$+\omega_1\alpha(\omega_1,t)g_2(\omega_2,t)-A(\omega_1)g_2(\omega_2,t)-h(\omega_1,\omega_2,t)\int A(\omega)\alpha(\omega,t)J(\omega)d\omega. \tag{22}$$

Now

$$p(t)=\frac{A_2(t)-B_2(t)}{A_2(t)+B_2(t)+2C_2(t)}, \tag{23}$$

where

$$A_2(t)=f_1(t)f_1^*(t)+f_1^*(t)\int h(\omega_1,\omega_2,t)\alpha^*(\omega_1,t)\alpha^*(\omega_2,t)J(\omega_1)J(\omega_2)d\omega_1d\omega_2+f_1(t)\int g_1^*(\omega,t)\alpha(\omega,t)J(\omega)d\omega$$
$$+f_1^*(t)\int g_1(\omega,t)\alpha^*(\omega,t)J(\omega)d\omega+\int g_1(\omega,t)g_1^*(\omega,t)J(\omega)d\omega+\int g_1^*(\omega_1,t)g_1(\omega_2,t)\alpha^*(\omega_2,t)\alpha(\omega_1,t)$$
$$\times J(\omega_1)J(\omega_2)d\omega_1d\omega_2+\int g_1^*(\omega_1,t)h(\omega_1,\omega_2,t)\alpha^*(\omega_2,t)J(\omega_1)J(\omega_2)d\omega_1d\omega_2+\int g_1^*(\omega_1,t)h(\omega_2,\omega_1,t)$$
$$\times\alpha^*(\omega_2,t)J(\omega_1)J(\omega_2)d\omega_1d\omega_2+\int g_1^*(\omega_1,t)h(\omega_2,\omega_3,t)\alpha^*(\omega_2,t)\alpha^*(\omega_3,t)\alpha(\omega_1,t)J(\omega_1)J(\omega_2)J(\omega_3)$$
$$\times d\omega_1d\omega_2d\omega_3+f_1(t)\int h^*(\omega_1,\omega_2,t)\alpha(\omega_1,t)\alpha(\omega_2,t)J(\omega_1)J(\omega_2)d\omega_1d\omega_2+\int h^*(\omega_1,\omega_2,t)g_1(\omega_2,t)$$
$$\times\alpha(\omega_1,t)J(\omega_1)J(\omega_2)d\omega_1d\omega_2+\int h^*(\omega_1,\omega_2,t)g_1(\omega_2,t)\alpha(\omega_2,t)J(\omega_1)J(\omega_2)d\omega_1d\omega_2+\int h^*(\omega_1,\omega_2,t)$$
$$\times g_1(\omega_3,t)\alpha^*(\omega_3,t)\alpha(\omega_1,t)\alpha(\omega_2,t)J(\omega_1)J(\omega_2)J(\omega_3)d\omega_1d\omega_2d\omega_3, \tag{24}$$

$$B_2(t)=A_2(f_1\rightarrow f_2,g_1\rightarrow g_2), \tag{25}$$

$$C_2(t)=2\Bigg[\int h^*(\omega_1,\omega_2,t)h(\omega_1,\omega_2,t)J(\omega_1)J(\omega_2)d\omega_1d\omega_2$$
$$+\int h^*(\omega_1,\omega_2,t)h(\omega_2,\omega_3,t)\alpha^*(\omega_3,t)\alpha(\omega_1,t)J(\omega_3)J(\omega_2)J(\omega_1)d\omega_1d\omega_2d\omega_3$$
$$+\int h^*(\omega_1,\omega_2,t)h(\omega_1,\omega_3,t)\alpha^*(\omega_3,t)\alpha(\omega_2,t)J(\omega_1)J(\omega_2)J(\omega_3)d\omega_1d\omega_2d\omega_3$$
$$+\int h^*(\omega_1,\omega_2,t)h(\omega_3,\omega_2,t)\alpha^*(\omega_3,t)\alpha(\omega_1,t)J(\omega_1,t)J(\omega_1)J(\omega_2)J(\omega_3)d\omega_1d\omega_2d\omega_3$$
$$+\int h^*(\omega_1,\omega_2,t)h(\omega_3,\omega_1,t)\alpha^*(\omega_3,t)\alpha(\omega_2,t)J(\omega_1)J(\omega_2)J(\omega_3)d\omega_1d\omega_2d\omega_3$$
$$+\int h^*(\omega_1,\omega_2,t)h(\omega_3,\omega_4,t)\alpha^*(\omega_3,t)\alpha^*(\omega_4,t)\alpha(\omega_1,t)\alpha(\omega_2,t)J(\omega_1)J(\omega_2)J(\omega_3)J(\omega_4)d\omega_1d\omega_2d\omega_3d\omega_4\Bigg]. \tag{26}$$

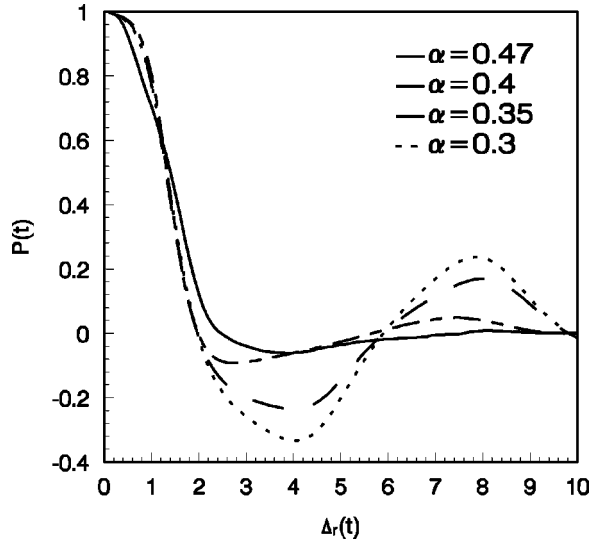

FIG. 2. Occupation probability for various damping; $\alpha<0.5$, $\Delta/\omega_c=1/50$, $\epsilon=0$.

Through the new state vector, we depict the numerical result for $p(t)$ at zero temperature and for small values $0<\alpha<0.5$ (Fig. 2). From Fig. 2 we can observe obvious coherent and damped oscillations. With the increase of α, quantum coherence becomes increasingly short-lived. However, the limitation of our method and accuracy of our data make it impossible for one to resolve oscillations of $p(t)$ for $\alpha>0.47$. From the obvious deviation of α_c that resulted from a different state vector it is clear that the second effect plays an important role in affecting the dynamical behavior of the system. An expanded view of decay of $p(t)$ in the vicinity of the critical value $\alpha_c=0.5$ is provided in Fig. 3. In this region, comparing results for different cutoff frequencies ω_c, we observe marked scaling behavior.

To investigate the energy transfer between the system and phonons, another quantity $N(t)=\langle\Sigma_i a_i^+ a_i\rangle$, excited phonon number, is calculated. Its numerical result is shown as Fig. 4.

When we associate Fig. 2 and Fig. 4 with Hamitonian (2), a clear energy transfer picture emerges. As the coupling

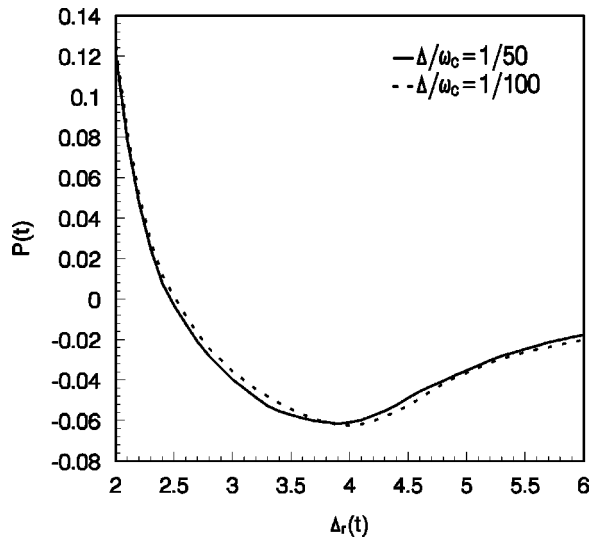

FIG. 3. Scaling behavior of the occupation probability for $\alpha=0.48$; $\epsilon=0$.

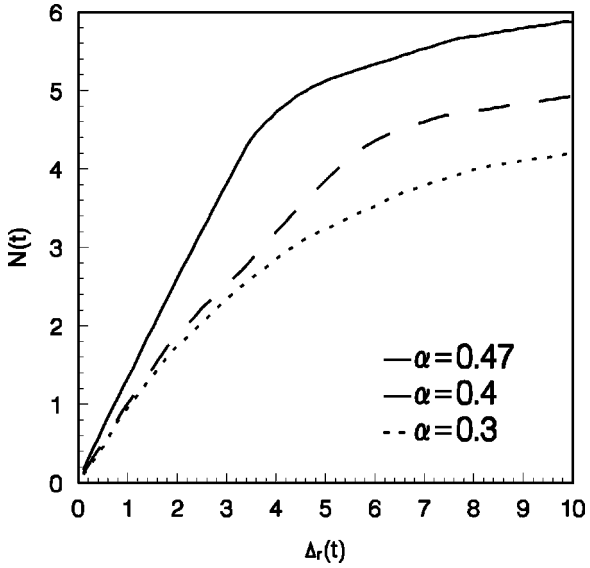

FIG. 4. The variation of phonon number for various damping; $\Delta/\omega_c=1/50$, $\epsilon=0$.

strength increases, the system energy decreases at a higher speed. At $\alpha=0.47$, the speed reaches its maximum. Likewise, the phonon number increases in the same pattern. As $t\to\infty$, the phonon bath gets to a new thermoequilibrium. Figure 2 just is the macroscopic correspondence to Fig. 4.

The phonon numbers $n(t)$ of three special frequencies are shown in Fig. 5. We notice that there exist great variations for different ω. At ω_c, the phonon number is almost zero. This result provides a reason for the high energy cutoff: near or above the ω_c, the phonon number is so small that its contribution to the dynamical behavior of the system can be neglected.

III. CONCLUSION

In conclusion, we have introduced a systematic approximate method for the dynamics of dissipative quantum sys-

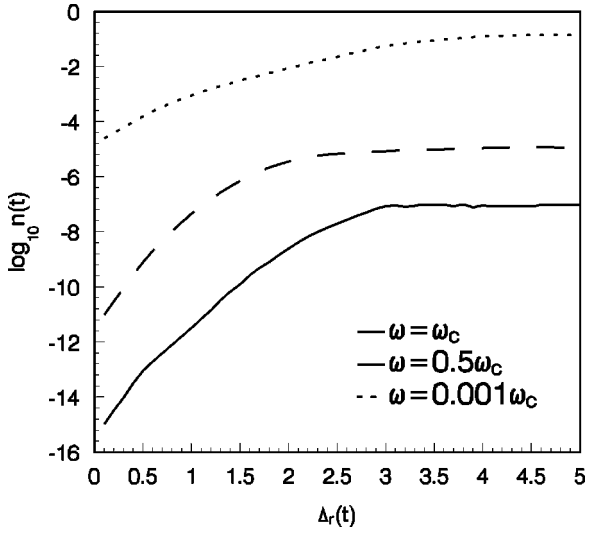

FIG. 5. A log plot of phonon number of three special frequencies versus $\Delta_r(t)$ for $\Delta/\omega_c=1/50$; $\alpha=0.47$, $\epsilon=0$.

tems and used it to explore the dynamical behavior, for the parameter range $\Delta/\omega_c = 50\,100$ at $0 < \alpha < 0.5$ without a bias. We found that the critical point at which coherent oscillation turns into incoherent exponential decay occurs in the vicinity of $\alpha_c = 0.5$. Most important, our method provides a microscopic decription for the dynamical behavior of this system: through spin-boson interaction, some bosons in the ground state are stimulated to excited states; the dissipative interaction causes the transition from two state to single state. It is expected that when the higher ($\geqslant 3$) order effect is added into the state vector, more accurate results will be obtained, and this process can be developed further indefinitely.

In view of the above, we can draw the conclusion that in the dissipative two-state system, our method is valid in small coupling, compared to the QMC or NIBA method. This might be useful for other quantum dissipative systems.

[1] B. Golding, N.M. Zimmerman, and S.N. Coppersmith, Phys. Rev. Lett. **68**, 998 (1992).
[2] S. Chakravarty and S. Kivelson, Phys. Rev. Lett. **50**, 1811 (1983).
[3] S. Chakravarty and A.J. Leggett, Phys. Rev. Lett. **52**, 5 (1984).
[4] A.J. Leggett, S. Chakravarty, A.T. Dorsey, M.P.A. Fisher, A. Garg, and W. Zwerger, Rev. Mod. Phys. **59**, 1 (1987); **67**, 725 (1995).
[5] H. Wipf, D. Steinbinder, K. Neumaier, P. Gutsmiedl, A. Magerl, and A.J. Dianoux, Europhys. Lett. **4**, 1379 (1987).
[6] S. Chakravarty and J. Rudnick, Phys. Rev. Lett. **75**, 501 (1995).
[7] T. A. Costi, Phys. Rev. Lett. **80**, 1038 (1998).
[8] S. Chakravarty, Phys. Rev. Lett. **49**, 681 (1982).
[9] A.J. Bray and M.A. Moore, Phys. Rev. Lett. **49**, 1545 (1982).
[10] J.W. Negele and H. Orland, in *Quantum Many-Particle Systems*, edited by D. Pines (Addison-Wesley, Reading, MA, 1987), p. 23.
[11] A. Garg, Phys. Rev. Lett. **77**, 964 (1996).
[12] Reinhold Egger, Hermann Grabbert, and Ulrich Weiss, Phys. Rev. E **55**, 3809 (1997).